ARMA 21–1103

Importance of block damage in confined laboratory-scale Bonded Block Model simulations

Sinha, S.
Colorado School of Mines, Golden, Colorado, United States
Walton, G.
Colorado School of Mines, Golden, Colorado, United States

This paper was prepared for presentation at the 55th US Rock Mechanics/Geomechanics Symposium held in Houston, Texas, USA, 20-23 June 2021. This paper was selected for presentation at the symposium by an ARMA Technical Program Committee based on a technical and critical review of the paper by a minimum of two technical reviewers. The material, as presented, does not necessarily reflect any position of ARMA, its officers, or members. Electronic reproduction, distribution, or storage of any part of this paper for commercial purposes without the written consent of ARMA is prohibited. Permission to reproduce in print is restricted to an abstract of not more than 200 words; illustrations may not be copied. The abstract must contain conspicuous acknowledgement of where and by whom the paper was presented.

ABSTRACT: Recent years have seen a rapid increase in the use of Bonded Block Models (BBM) for studying the rock fracturing process, both at the laboratory-scale and at the field-scale. In laboratory-scale BBMs, the blocks are analogous to constituent mineral grains while the contacts between neighboring blocks correspond to grain boundaries. It is known that during a compression test on granite, heterogeneity-driven pre-peak damage initiates first along grain boundaries, but as the load is increased up to and beyond peak, intragranular fracturing starts to play an increasingly important role. This is especially true in triaxial tests where the confining stress suppresses the formation of local tensile stresses within a specimen. It follows that a BBM developed to simulate rock behaviors over a wide range of confinements should allow for both grain boundary cracking as well as cracking or damage within the grains (or blocks). Since grain boundary cracking is an inherent feature of BBMs, this study instead focuses on the approaches for simulating the grain damage process. In particular, grain damage in UDEC BBMs can be explicitly modeled by introducing failure pathways within each block or it can be implicitly modeled using inelastic blocks. To identify which of the two approaches is superior from a phenomenological and a computational standpoint, a comparison is made between an elastic BBM (no grain damage), an inelastic BBM and an elastic BBM with explicit fractures within each block in terms of their ability to reproduce the geomechanical attributes (unconfined and confined) of a granitic rock. It was found that the elastic BBM with no provision for grain damage overpredicted the peak strengths for high confinement conditions. The introduction of inelasticity or explicit fractures within the blocks, both led to a good match in peak strengths for the entire range of confining stresses tested, although the latter failed to properly replicate the confinement dependency of peak dilation angle and the post-peak response.

1. INTRODUCTION

Damage in brittle crystalline rocks (e.g., granites) under compression begins with grain boundary cracking, followed by growth and coalescence of these microcracks that ultimately leads to the formation of a macroscopic shear band (Bieniawski, 1967; Martin and Chandler, 1994). Understanding and advancing our knowledge of this damage process under confined and unconfined conditions is a pre-requisite for predicting the behavior of underground structures like tunnels, mine opening, etc. While non-invasive characterization tools like Digital Image Correlation, acoustic emission and ultrasonic monitoring are powerful techniques, they cannot provide complete information regarding the progressive fracturing process. To better understand these processes, one can use an appropriately constrained and calibrated numerical model developed using the Bonded Block Modeling (BBM) approach, a sub-class of the Discrete Element Method (DEM), which has found wide applications in recent years (Preston et al., 2013; Li et al., 2017; Stavrou and Murphy, 2018; Sinha and Walton, 2019a; Sinha et al., 2020). The current study specifically deals with the polygonal BBM approach as implemented in the Itasca software Universal Distinct Element Code or UDEC.

In a UDEC BBM, a material space is partitioned into triangular (called ‘Trigons’) or polygonal (typically ‘Voronoi’) blocks, and each block can interact with its neighboring blocks per a pre-defined contact algorithm. The discontinuum nature of UDEC allows the blocks to detach completely once the tensile and/or shear strength of a given contact is exceeded. The Voronoi BBM approach has become widely accepted for simulating crystalline rocks because of the resemblance in the block shape to actual mineral grains. In context of rock microstructure, each block therefore corresponds to a constituent mineral grain, while each contact represents a grain boundary. The blocks in a UDEC BBM can be made elastic or inelastic, depending on the constitutive model assigned to the finite difference zones within each block.

Previous laboratory and numerical-based studies have indicated that grain boundary cracking is the predominant damage mode under unconfined conditions; as the confinement on the rock specimen is increased, intergranular fracturing starts to play an increasingly important role (Sprunt and Brace, 1974; Tapponnier and Brace, 1976; Kranz, 1983; Hofmann et al., 2015; Peng et al., 2018; Abdelaziz et al., 2018). This is especially true in granitic rocks that are composed of different mineral grains. Irrespective of the applied confinement, grain boundary cracking initiates first in the pre-peak portion of the stress-strain curve due to the elastic mismatch between the mineral grains. With continued loading, either the grain boundary cracks grow and coalesce into a macroscopic axial fracture (unconfined/low confinements) or they interact via intragranular fractures to form a shear band (moderate/high confinements). It follows that if rock behaviors over a wide range of confinement are to be simulated, then a reasonable approximation of grain boundary cracking and intragranular fracturing is necessary.

Grain boundaries are an inherent feature of laboratory-scale polygonal BBMs, and damage to these boundaries represents intergranular cracking. There is, however, no consensus regarding the best approach to simulate intragranular fracturing, with most previous studies neglecting this damage mechanism by employing unbreakable, elastic blocks. It is noted here that once a block is discretized by constant-strain zones and the model is cycled, UDEC does not allow further partitioning/breakage of blocks. With that in mind, there are two main approaches that can be used to simulate the intragranular fracturing process:

(1) **Explicit** – In this approach, additional contacts are incorporated within each block (to form sub-blocks) prior to meshing, such that these contacts can act as intra-block failure pathways. Gao et al. (2016) and Wang and Cai (2018) have previously used this approach to model a sandstone and a granite, respectively. The major disadvantages are the increase in model runtime due to the increase in number of blocks, and the enforcement of kinematic constraints on where a fracture can develop when a small number of sub-blocks (i.e. ~5-6/block) is used.

    In general, the runtime of a UDEC model is a function of both the number of gridpoints (vertices of zones) in blocks, and the number of contacts in a model. If there are very few contacts in the model, then the time is proportional to $N^{3/2}$, where N is the number of gridpoints in blocks (Itasca, 2014). This formula holds for elastic problems. The runtime will vary somewhat, but not substantially, for plasticity problems.

(2) **Implicit** – Where it is not computationally feasible to generate a large number of sub-blocks, a potential alternative is to utilize continuum zones with an inelastic constitutive model (Sinha and Walton, 2020). Specifically, a strain-softening Mohr-Coulomb model can be used to approximate the loss of load-carrying capacity of mineral grains induced by fracturing. This is an implicit approach for simulating the intragranular fracturing process, and it does not increase the model runtime relative to an elastic block model significantly.

This study compares the capabilities of BBMs with elastic blocks (only grain boundary cracking), inelastic blocks (implicit intragranular fracturing) and elastic blocks with fractures (explicit intragranular fracturing) to reproduce a wide range of rock mechanical attributes for a granitic rock. Special attention was paid to mechanical behavior under confined conditions, where intragranular fracturing is known to play an important role in the overall rock damage and deformation process. The ability of a UDEC BBM to reproduce different mechanisms depends on model setup decisions, and because these micromechanical models are physics-based, it is generally possible to identify physical reasons whenever an aspect of rock behavior cannot be replicated by a given model. These phenomenological reasons will be discussed throughout the body of the paper. Ultimately, this study has the potential to help future researchers in choosing a BBM representation that is appropriate for simulating rock behaviors over a wide range of confinements. It is important to note here that since the physical processes that occur in this granite may not be representative of those that occur in more porous and/or homogeneous rocks, the conclusions drawn may not apply equally well to such rocks.

2. ROCK DESCRIPTION AND MODEL SETUP

The rock considered in this study is “Creighton Granite”, which is a granitic rock from Sudbury, Canada. It is composed of approximately 15% Biotite, 30% Quartz and 55% Na-Feldspar and has an average grain size of 2.25 mm (Sinha and Walton, 2019b). Geomechanical characterization of this rock was previously conducted by Walton et al. (2016) based on uniaxial and triaxial (confining stress range of 0-60 MPa) compression test data from laboratory. Besides the peak strengths, Crack Initiation (CI) thresholds, Crack Damage (CD) thresholds and volumetric changes in the rock specimens were also examined in detail by Walton et al. (2016).

Recently, the authors attempted to model this rock type using different representations of blocks, zones and contacts (Sinha and Walton, 2020). In particular, different combinations of homogeneous and heterogeneous (corresponding to different mineral grains and associated

mechanical properties) blocks, homogeneous and heterogeneous contacts, and elastic and inelastic zones were tested. Heterogeneity was found to be an important feature for capturing the pre-peak damage thresholds (CI and CD; discussed later) in a multiminerallic rock like granite, and hence homogeneous BBMs are not considered here. Some of the models described in this study are taken directly from the aforementioned comprehensive complexity analysis; interested readers are referred to Sinha and Walton (2020) for detailed discussion on this analysis and the calibration process. These are then compared to the BBMs with explicit intragranular fracturing developed for this study.

For the UCS simulation, a rectangular model of 120 mm x 55 mm was developed and was loaded via a constant velocity along the top surface (Figure 1). The bottom was constrained with roller boundaries. Triaxial simulations were also conducted using the same model setup, but with a stress boundary along the lateral edges of the model. The Brazilian sample was 55 mm in diameter and loaded through two steel platens on either side (Figure 1). Three sets of properties, corresponding to the three mineral grains, were assigned to the blocks in the areal proportions of Creighton Granite as defined above. This also included six sets of contact properties corresponding to the different mineral grain associations. The mineral elastic properties were chosen from Bass (1995) and Mavko et al. (2009). For the inelastic zone representation, a strain-softening constitutive model was considered to mimic the loss of load carrying capacity of damaged/ microfractured mineral grains.

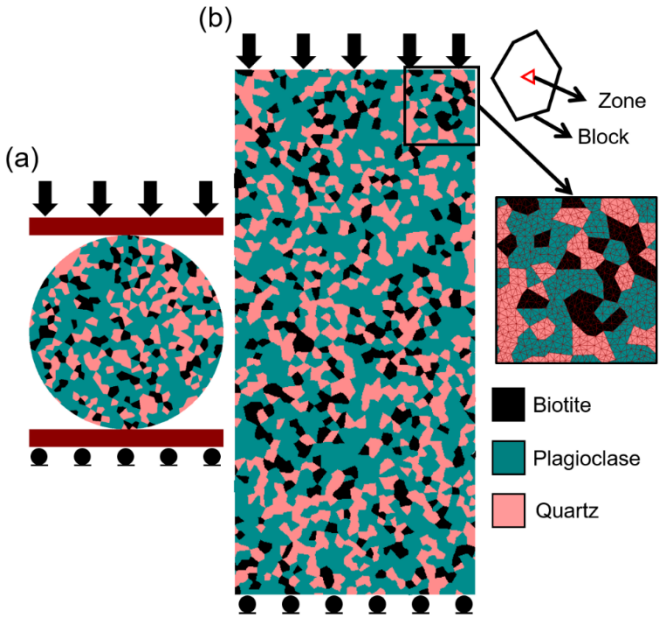

Fig 1. BBM model setup for (a) Brazilian Tensile Strength test, (b) UCS / triaxial test (after Sinha et al., 2020).

In the explicit intra-block fracturing model, each mineral block was further divided into sub-blocks. Sub-blocks were generated by determining the centroid of each block and then incorporating crack elements between the centroid and the block vertices. A similar methodology was followed by Gao et al. (2016) for creating sub-tessellations in their Voronoi models. As each sub-block was further discretized using constant strain-triangular zones, a criterion was set in order to prevent creation of very small sub-blocks – smaller sub-blocks would require smaller zones, which would ultimately increase the model run-time. In particular, the crack insertion procedure was skipped whenever the distance between the centroid and a vertex was less than 0.75 mm. Figure 2 shows the final geometry of the model. Care was taken to not modify the block structure or the location of each mineral block within the model such that a direct comparison with the heterogeneous, elastic BBM is possible.

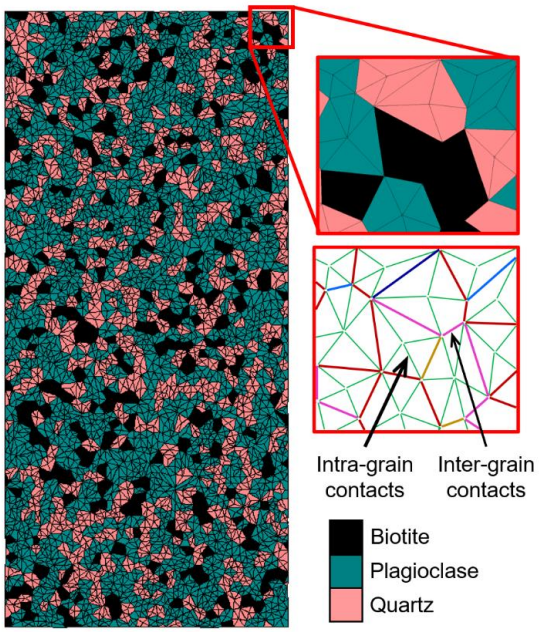

Fig 2. Geometry of small-scale BBM with explicit intra-grain contacts.

It is important to record the axial stress and strain and lateral strain during the simulations so as to be able to compare the model-derived attributes to those from laboratory. For that purpose, the displacements along all gridpoints along the top/bottom edges and 10 pairs of gridpoints along the lateral edges of the model were tracked – these were later converted to axial and lateral strains by dividing with the length and width of the model, respectively. Axial stress was computed by dividing the sum of the unbalanced forces at all gridpoints along the model top with the width of the model. The extractions were performed once every 1000 solution steps using user-defined FISH functions.

Before presenting the results, the input parameters used for the different models are briefly summarized. In all three model types, the contacts are defined by normal and shear stiffness, peak and residual cohesion, peak and residual friction angle and peak and residual tensile

strength. If blocks are elastic, then their behavior is defined fully by density, bulk modulus and shear modulus; if inelastic, then block strength parameters like peak and residual cohesion, peak and residual friction angle, peak and residual tensile strength and critical plastic shear strain need to be defined. The parameters for the 'explicit' model are given in this study while the outstanding ones can be found elsewhere (Sinha and Walton, 2020).

3. HETEROGENEOUS, ELASTIC BBM

The heterogeneous, elastic representation has no provision for intra-block damage, and fracturing can only occur along the block boundaries. Since the intragranular damage process is neglected, one can expect the model to be incapable of completely reproducing the high confinement attributes of rock.

Figure 3 compares some laboratory-measured properties of Creighton Granite with those predicted by the calibrated model. The target elastic constants, which were calculated as an average over all confinements, effectively ignoring the confinement-dependency present in some of the laboratory data due to the presence of pre-existing fractures, were well captured (Sinha and Walton, 2020). Volumetric strain in Figure 3e was determined per the equation: Volumetric strain = Axial strain + 2*Lateral strain, with negative strain implying extension. The calculation of the peak dilation angle required determining instantaneous dilation angles at numerous points along the stress-strain curves and then identifying the maximum value (Sinha and Walton, 2020). The maximum dilation angles normalized by the maximum dilation angle for the UCS simulation are shown in Figure 3f; the decreasing trend in the laboratory data signifies a change in the mode of fracture formation from highly dilatant extensile (axial) cracking to medium-low dilation shear (oblique) cracking as the confining pressure on the specimen is increased (Walton and Diederichs, 2015).

CI and CD are pre-peak damage thresholds, and they represent the onset of extensile and shear microcracking in the rock specimen, respectively. Sinha & Walton (2020) showed that by incorporating heterogeneity, these thresholds could be matched across a wide range of confinements (see Figure 3c and d).

Some interesting observations can be made from Figures 3 (a-d). Even though the BBM was able to match the pre-peak damage thresholds, the peak strengths for σ_3 = 40 & 60 MPa were slightly overestimated. This occurred because at CI and CD, damage is mostly restricted to grain boundaries; intragranular cracking is only appreciable when loading continues past CD and into the post-peak. Additionally, the contribution of intragranular cracking in the CD to peak stress range is more important under moderate to high confinement conditions (Abdelaziz et al., 2018; Sinha, 2020). Since the heterogeneous, elastic BBM did not allow block damage, grain boundary fractures could not connect via intragranular fractures and a longer fracture path along the block boundaries had to be followed. This ultimately manifested in an extended pre-peak hardening phase, as shown in Figure 3a. Note the tendency of elastic BBMs to yield a near-linear strength envelope in σ_1 - σ_3 space, even though the actual laboratory trend is non-linear (convex).

In addition to the previously identified mismatches, the post-peak response was also somewhat unrealistic, in that the stresses rapidly dropped to low values rather than declining gradually to residual levels. Again, this is a behavior typical of elastic BBMs (Chen et al., 2016). It appears that the lack of block damage is responsible for the over-prediction of the σ_3 = 40 & 60 MPa strengths as well as the mismatch in the post-peak behavior.

Lastly, the confinement-dependent dilatancy phenomenon was well represented by the models. The data-model discrepancy at higher confinements (Figure 3f) can be attributed to the lack of intragranular fracturing, pervasive contact failure in the BBMs and the ability of block contacts to dilate excessively (related to the polygonal block shape). Because the minimally dilatant intragranular shearing mechanism was not simulated in this BBM, an overestimation of volume changes at higher confinements is not surprising.

4. HETEROGENEOUS, INELASTIC BBM

The heterogeneous, inelastic BBM mimics the intra-block damage process through inelastic softening of zones and is an implicit approach in that no actual intra-block fractures are present in the model. This approximation is justified only when the mechanism under consideration exhibits limited dilatancy (so that is can be modeled as a continuum), as is the case with intragranular fracturing. The inelastic BBM approach also has the potential to be used in the design of rock pillars, where highly dilatant peripheral fracturing can be modeled explicitly via contact damage and minimally dilatant shearing within the confined core can be simulated as zone yield (Sinha and Walton, 2021).

Figure 4 shows the results of the calibrated BBM that could match all known rock mechanical attributes of Creighton Granite. The models were able to reproduce the target Young's modulus and Poisson's ratio very well (Sinha and Walton, 2020). The stress-strain curves are relatively brittle, with modest pre-peak hardening (Figure 4a) and are generally consistent with the laboratory data. Unlike the elastic BBM, the non-linear trend of the peak strength envelope is reproduced (Figure 4b). Lastly, the CI and CD thresholds (Sinha et al., 2020), normalized peak dilation angle and volume change in the specimen

were all replicated (Figure 4c, d); this highlights the well-calibrated nature of the BBM.

Inelastic yield was minimal in the UCS simulation and initiated only after CD in the confined models, with the intensity and distribution increasing as a function of confining pressure. The major effect of inelasticity was to reduce the extent of pre-peak hardening and raising the drop modulus (brittleness) and residual stress levels. With all that in mind, it seems that the heterogeneous, inelastic representation is appropriate for simulating the full range of rock behavior.

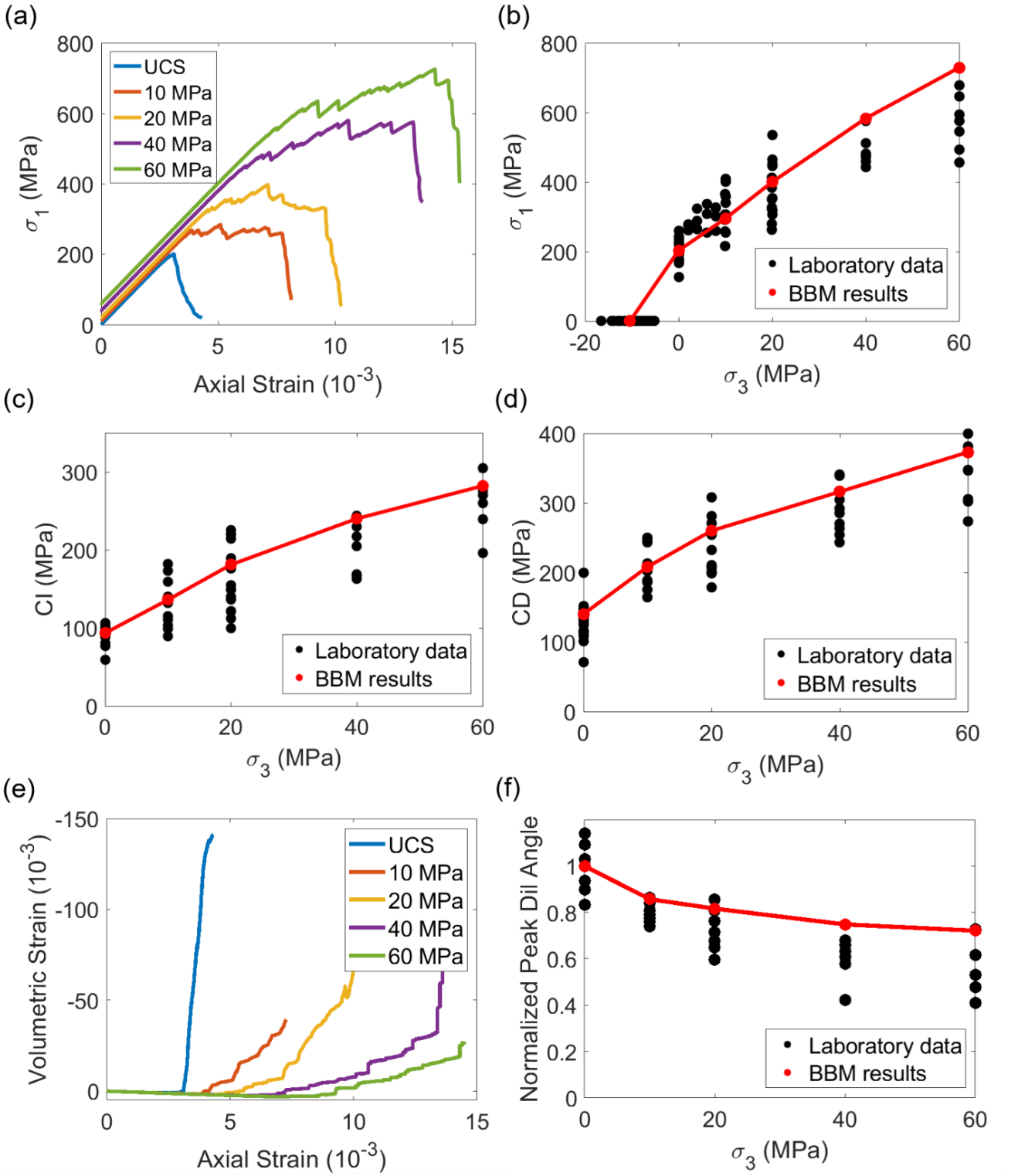

Fig 3. Heterogeneous, elastic BBM results: (a) Stress-strain curves for 0-60 MPa confinement, (b) Model strengths in σ_1 - σ_3 space, (c) CI thresholds, (d) CD thresholds, (e) Volumetric strain - axial strain, (f) Normalized peak dilation angle versus confinement (after Sinha and Walton, 2020).

An interesting observation was made during the calibration of the heterogeneous, inelastic BBM. Initially, the model was calibrated considering three different sets of inelastic parameters for the three constituent mineral phases, but when the same model was run with one set of inelastic properties (derived by area-weighted average of the inelastic strength parameters for the three mineral grains; see Table 1), it performed equally well in replicating the calibration targets (Figure 5). Since both BBMs behaved similarly, the homogenized inelastic zone property model was ultimately employed. Given that rock mechanics problems are generally data-limited, researchers must always strive to identify the lowest model complexity level possible that can simulate the target mechanics (Starfield and Cundall, 1988).

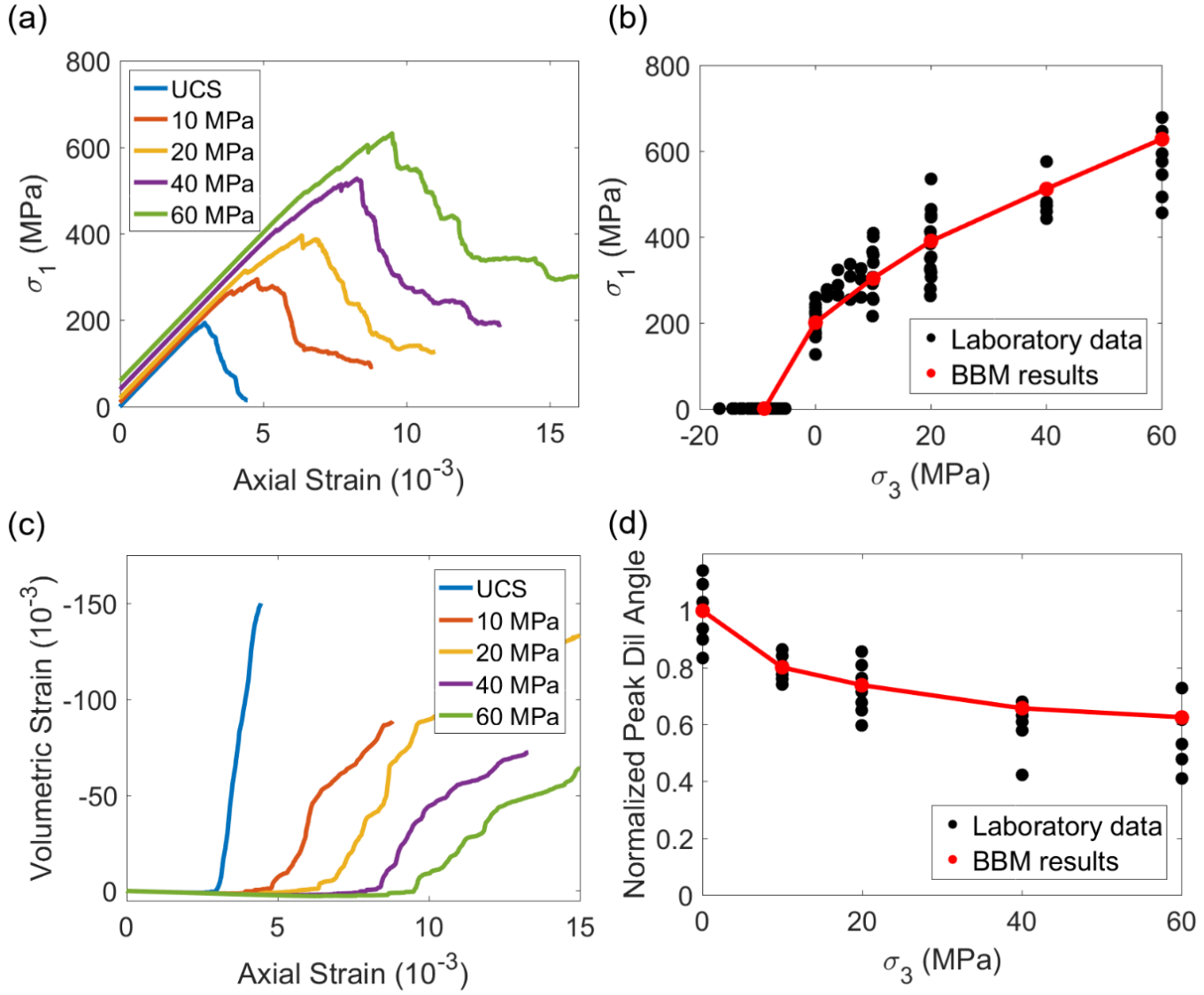

Fig 4. Heterogeneous, inelastic BBM results: (a) Stress-strain curves for 0-60 MPa confinement, (b) Model strengths in σ_1- σ_3 space, (c) Volumetric strain - axial strain, (d) Normalized peak dilation angle versus confinement (after Sinha and Walton, 2020).

Table 1. Strain-softening zone parameters for the 'Het Inelas.' and 'Homo Inelas.' BBMs. 'Homo Inelas' has only one parameter set as the same inelastic properties were assigned to all mineral blocks.

Model	Mineral Type	Proportion (%)	Cohesion (MPa)		Friction angle (deg)		Tensile strength (MPa)	
			Peak (c_{peak})	Residual (c_{res})	Peak (φ_{peak})	Residual (ϕ_{res})	Peak ($\sigma_{t,peak}$)	Residual ($\sigma_{t,res}$)
Het Inelas.	Plagioclase	55	120	50	68	50	50	0
	Quartz	30	130	50	68	50	60	0
	Biotite	15	90	40	48	35	40	0
Homo Inelas.	N/A - Homogenized	100	118.5	48.5	65	47.8	51.5	0

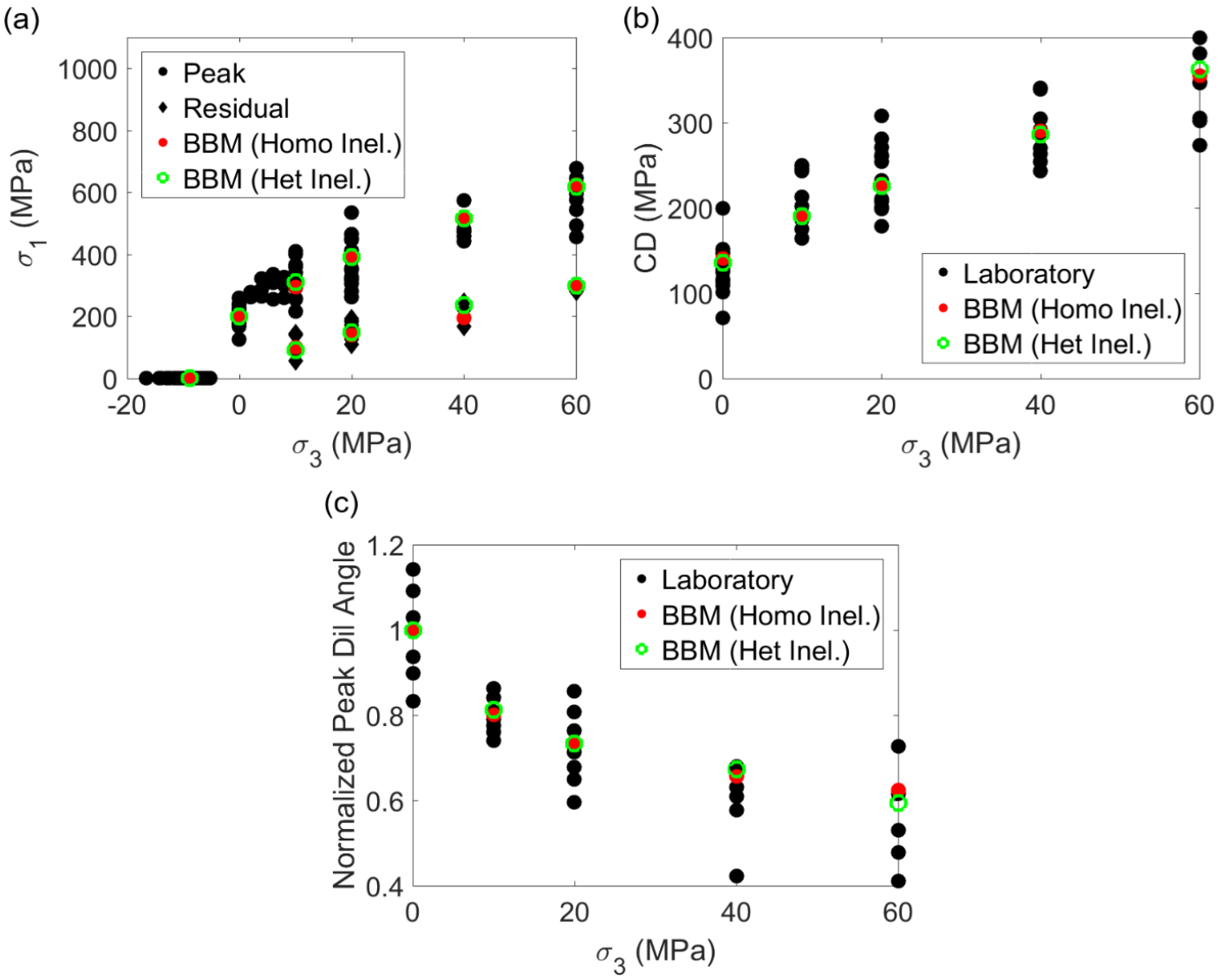

Fig 5. (a) Comparison of model and laboratory peak and residual strength, (b) Comparison of model and laboratory CD thresholds, and (c) Comparison of model and laboratory normalized peak dilation angle. 'Homo Inel.' refers to the BBM with only one set of inelastic parameters (results shown in Figure 4 correspond to this model) while 'Het Inel.' refers to the BBM with three different sets of inelastic parameters.

5. HETEROGENEOUS, ELASTIC BBM WITH INTRA-BLOCK FRACTURES

In the explicit intra-block fracture BBM, the same inter-grain contact properties as those in the heterogeneous, elastic BBM were selected and only the intra-grain contact properties were modified. The goal of this modeling exercise was three-fold: (1) Determine if the high confinement peak strengths could be reproduced if intragranular fracturing was considered explicitly, (2) Discern if the excessive pre-peak hardening in the stress-strain curves for the heterogeneous, elastic BBMs could be reduced by providing additional pathways for fracture development, and, (3) Identify whether behaviors similar to the heterogeneous, inelastic BBM could be obtained using such an approach. Note that each sub-block in this BBM was modeled as elastic, meaning that damage could occur only along the inter- (i.e. grain boundary) and intra-grain contacts.

Table 2 lists the calibrated set of intra-grain contact properties. Very high values had to be selected to allow damage to initiate first at grain boundaries, followed by grain damage at higher stress levels. All intra-grain contacts were assigned the same properties in order to reduce the potential for parameter non-uniqueness, and also because a single set of inelastic properties (for all grains in the model) could sufficiently reproduce various pre- and post-peak geomechanical attributes. When calibrating the models, it was found that the intra-grain contacts had a predisposition to fail in tension. Consequently, tensile strength that was much higher than the cohesive strength had to be selected. Such cohesion to tensile strength ratio for intra-grain properties was also used by Hoffman et al. (2015).

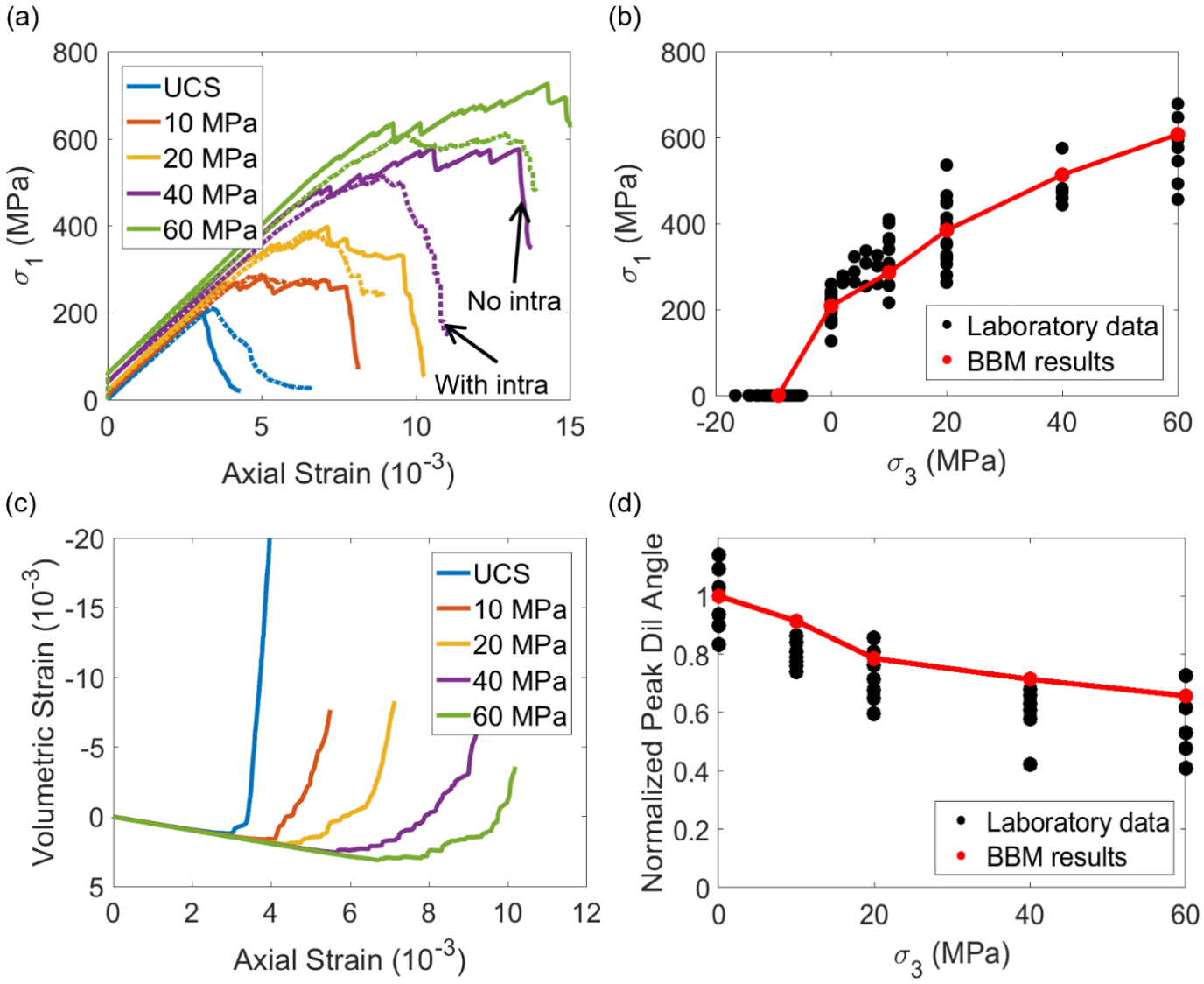

Fig 6. Heterogeneous, elastic BBM (explicit intragranular fracture) results: (a) Comparison of stress-strain curves of models with and without intragranular fracturing capability, (b) Comparison of peak strength as measured in laboratory and as obtained from the BBM, (c) Volumetric strain versus axial strain from the BBM, (d) Normalized peak dilation angle versus confinement.

Table 2. Calibrated parameter set of the intra-grain contacts.

Parameters	Normal stiffness (GPa/m/m)	Normal stiffness/ Shear stiffness	Peak cohesion* (MPa)	Peak friction angle (°)	Residual friction angle (°)	Peak tensile strength* (MPa)
Values	800,000	2	210	72.5	5	380

*Residual values are set to zero.

Figure 6a shows the model-predicted peak strengths as compared to the laboratory data. It can be observed that the BBM was capable of reproducing the peak strengths for the entire range of confinement tested (as well as the tensile strength). Also note the non-linear shape of the BBM strength envelope, in contrast to the elastic BBM (without intragranular fracturing). Figure 6b shows the stress-strain curves for σ_3 = 0-60 MPa simulations with and without intragranular fracturing capability. The stress-strain responses are smoother and more realistic for the current set of models in comparison to the elastic BBM without intra-grain contacts. Based on these results, it can be stated that enabling damage to develop within the grains themselves significantly improved the phenomenological capabilities of the BBM.

The specimen Young's modulus values for these models are lower (~10%) than for the models without intra-grain contacts (Figure 6b). This occurred because of the greater number of contacts in the model. Even though the joint normal and shear stiffnesses of the intra-grain contacts

were assigned much higher values than those at the grain boundaries, a drop in the elastic modulus still occurred. Further increasing the stiffnesses could have resulted in higher modulus values, but at the expense of longer runtime (timestep is inversely related to the stiffness of various components in an UDEC model). The post-peak responses could not be obtained due to contact overlap and block deformation errors. This problem occurred with almost all parameter sets tested as a part of this study. These results suggest that the post-peak behaviors can be better reproduced when using inelastic zones within the blocks.

A major point of discrepancy relative to the laboratory data is the overestimation of normalized peak dilation angle for almost the entire range of confinement tested (Figure 6d). To understand the cause of this discrepancy, the average laboratory volumetric strain curves were overlaid with those from the explicit and implicit BBMs and are shown in Figure 7. In this graph, the slope of the straight segment (refer to the black dashed lines) for the explicit UCS model is lower than those of the implicit model and laboratory data, meaning that the peak dilation angle is lower in the explicit model. Since the datapoints in Figure 6d were normalized with respect to the peak unconfined dilation angle, a relative overestimation for the other confining stresses occurred.

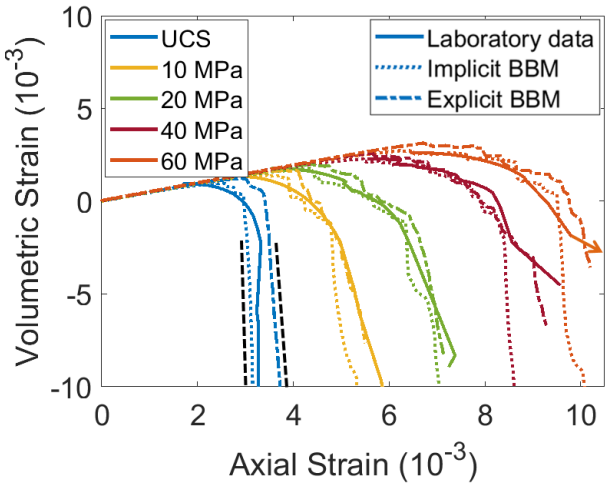

Fig 7. Comparison of volumetric strains in the explicit and implicit BBMs with the laboratory data.

A plausible physical explanation for the aforementioned discrepancy could be the breakage of the polygonal grains into trigons at late stages of loading, meaning that the high dilatancy associated with polygonal block movements under unconfined/low confinement conditions was to some extent substituted by minimally dilatant shear between trigon blocks (Figure 8; Sinha and Walton, 2019a). In the heterogeneous, inelastic BBM, the grains remained intact, and therefore the large dilatancy induced by block movements was preserved. A similar finding was noted in field-scale simulations by Sinha and Walton (2021), where a pillar with explicit intra-block fracturing capability was successful in matching the target peak strengths, but underestimated dilatancy near the pillar edges (low confinement condition). It is interesting that the explicit BBM matched the σ_3 = 40 MPa & 60 MPa volumetric strains so well (Figure 7), perhaps because the damage at such high confinements is minimally dilatant and trigons are better suited for simulating such behavior.

Although the implicit model performed better in reproducing the normalized peak dilation angle values, both models exhibit notable errors in capturing the decay in dilation angle with continued damage. The explicit model, in fact, outperformed the implicit one slightly for the σ_3 = 40 MPa & 60 MPa simulations. The decay in dilatancy with damage cannot be completely modeled because the process of asperity degradation along the macroscopic shear band that forms under such confinement conditions is not considered in these micromechanical models (Walton and Diederichs, 2015; Sinha et al., 2020).

Overall, using inelastic zones to simulate the grain damage process seems to be a preferable approach both from a computational and a mechanistic standpoint. The model runtime for the explicit BBMs ranged from 5-10 days (confined simulations took longer) while all implicit models finished running within ~1.5 days on an Intel Core i7-6950X, 3.0 GHz, 64 GB RAM workstation. Where replication of the details of the post-peak response is not of particular concern, the explicit approach could be used, however.

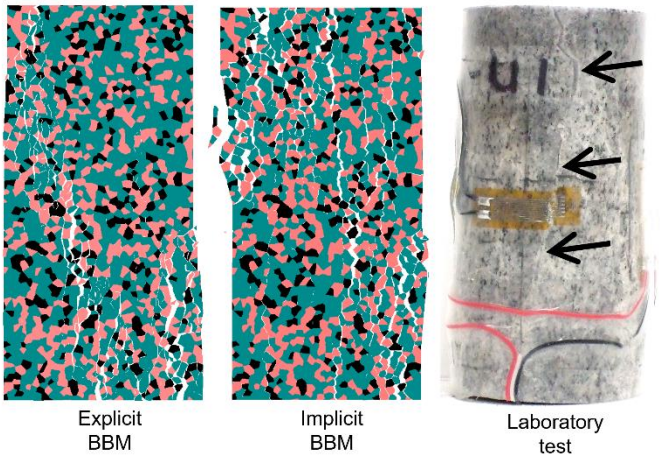

Fig 8. Fracture pattern for the UCS simulation using the explicit and implicit approaches. A laboratory specimen is shown here for reference. Note the axial cracks indicated by the arrows, and their similarity with those obtained from the simulations.

6. CONCLUSIONS

This study has highlighted the need to allow block damage in laboratory-scale UDEC BBMs for simulating confined rock attributes of a granitic rock and has also contrasted the implicit (grain damage is approximated by inelastic continuum yield) and explicit (grain damage is

simulated by actual fracture development within a block) approaches for simulating the intragranular fracturing process. The following conclusions were drawn:

(1) The application of BBMs with no provision for block damage should be restricted to studying rock behavior under low-moderate confinement conditions only. If high confinement is applied to such models, then excessive pre-peak hardening, and overestimation of peak strengths and specimen dilatancy under confined conditions occurs. Post-peak responses are also unrealistic, as intragranular fracturing is an important post-peak damage mechanism in reality.

(2) The implicit model could match all target attributes for the entire range of confinement tested. These models even captured the convex shape of the peak strength envelope and the confinement-dependent dilatancy phenomenon. This approach is robust for simulating the full range of rock behavior.

(3) The explicit model also yielded a convex peak strength envelope and matched all pre-peak damage thresholds. This representation, however, could not properly replicate the confinement dependency of peak dilation angle and the post-peak response. The former was attributed to the underestimation of the peak dilation angle for unconfined condition due to breakage of the polygonal blocks into trigons (trigon movements are less dilatant in comparison to polygonal block movements). The latter was attributed again to the elastic nature of the blocks. If post-peak response is not of particular interest, then this approach could be employed for micromechanical simulations.

(4) Both the implicit and explicit model could not simulate the decay in dilatancy with continued damage at higher confinements because the asperity degradation process was not considered in these models.

(5) The explicit approach is computationally intensive, with simulations taking over than 3 times longer to complete in comparison to the corresponding implicit models. The implicit approach is therefore advantageous from a practical application standpoint.

(6) The conclusions drawn may not be equally applicable to porous and/or homogeneous rocks as the microdamage processes are likely different than those in granites.

ACKNOWLEDGEMENT

The research conducted for this study was funded by the National Institute for Occupational Safety and Health (NIOSH) under Grant Number 200-2016-90154. The authors would like to extend their gratitude for the financial support. The modeling effort for this study was conducted using educational licenses of UDEC provided by Itasca Consulting, Ltd. The authors appreciate Itasca's support in this capacity.

REFERENCES

1. Abdelaziz, A., Q. Zhao, and G. Grasselli. 2018. Grain based modelling of rocks using the combined finite-discrete element method. *Computers and Geotechnics*. 103: 73-81.
2. Bass, J.D. 1995. Elasticity of minerals, glasses, and melts. *Mineral physics and crystallography: A handbook of physical constants*. 2: 45-63.
3. Bieniawski, Z.T. 1967. Mechanism of brittle fracture of rock: part I—theory of the fracture process. *International Journal of Rock Mechanics and Mining Sciences and Geomechanics Abstracts*. 4(4): 395-406.
4. Chen, W., H. Konietzky, X. Tan, and T. Frühwirt. 2016. Pre-failure damage analysis for brittle rocks under triaxial compression. *Computers and Geotechnics*. 74: 45-55.
5. Gao, F., D. Stead, and D. Elmo. 2016. Numerical simulation of microstructure of brittle rock using a grain-breakable distinct element grain-based model. *Computers and Geotechnics*. 78: 203-217.
6. Hofmann, H., T. Babadagli, J.S. Yoon, A. Zang, and G. Zimmermann. 2015. A grain based modeling study of mineralogical factors affecting strength, elastic behavior and micro fracture development during compression tests in granites. *Engineering Fracture Mechanics*. 147: 261-275.
7. Itasca. 2014. *UDEC Version 6.0: Theory and Background*. Itasca Consulting Group Inc., Minneapolis, Minnesota.
8. Kranz, R.L. 1983. Microcracks in rocks: a review. *Tectonophysics*. 100(1-3): 449-80.
9. Li, J., H. Konietzky, and T. Frühwirt. 2017. Voronoi-based DEM simulation approach for sandstone considering grain structure and pore size. *Rock Mechanics and Rock Engineering*. 50(10): 2749-61.
10. Martin, C.D., and N.A. Chandler. 1994. The progressive fracture of Lac Du Bonnet granite. *International Journal of Rock Mechanics and Mining Sciences and Geomechanical Abstracts*. 31(6): 643–659.
11. Mavko, G., T. Mukerji, and J. Dvorkin. 2009. *The rock physics handbook: Tools for seismic analysis of porous media*. Cambridge university press.
12. Peng, J., L.N. Wong, C.I. The, and Z. Li. 2018. Modeling micro-cracking behavior of Bukit Timah granite using grain-based model. *Rock Mechanics and Rock Engineering*. 51(1): 135-154.
13. Preston, R.P., D. Stead, H. McIntire, and D.P. Roberts. 2013. Quantifying the effects of adverse geology on pillar

strength through numerical modeling. Proceedings of the *47th US Rock Mechanics/ Geomechanics Symposium*, San Francisco, California, US. Paper No. 478.

14. Sinha, S., and G. Walton. 2019a. Understanding continuum and discontinuum models of rock-support interaction for excavations undergoing stress-induced spalling. *International Journal of Rock Mechanics and Mining Sciences*. 123: 104089.
15. Sinha, S., and G. Walton. 2019b.imulating laboratory-scale damage in granite using Bonded Block Models (BBM). Proceedings of the *14th International Congress on Rock Mechanics and Rock Engineering*, Foz do Iguassu, Brazil. 2461-2468.
16. Sinha, S., D. Shirole, and G. Walton. 2020. Investigation of the micromechanical damage process in a granitic rock using an inelastic bonded block model (BBM). *Journal of Geophysical Research: Solid Earth*. 124.
17. Sinha, S. 2020. *Advancing continuum and discontinuum models of brittle rock damage and rock-support interaction*. Ph.D. Thesis, Colorado School of Mines, Golden, Colorado.
18. Sinha, S., and G. Walton. 2021. Investigation of pillar damage mechanisms and rock-support interaction using Bonded Block Models. *International Journal of Rock Mechanics and Mining Sciences*. 104652.
19. Sprunt, E.S., and W.F. Brace. 1974. Direct observation of microcavities in crystalline rocks. *International Journal of Rock Mechanics and Mining Sciences and Geomechanics Abstracts*. 11(4): 139-150.
20. Starfield, A.M., and P.A. Cundall. 1988. Towards a methodology for rock mechanics modelling. *International Journal of Rock Mechanics and Mining Sciences and Geomechanical Abstracts*. 25(3): 99-106.
21. Stavrou, A., and W. Murphy. 2018. Quantifying the effects of scale and heterogeneity on the confined strength of micro-defected rocks. *International Journal of Rock Mechanics and Mining Sciences*. 102: 131-43.
22. Tapponnier, P., and W.F. Brace. 1976. Development of stress-induced microcracks in Westerly granite. *International Journal of Rock Mechanics and Mining Sciences & Geomechanics Abstracts*. 13(4): 103-112.
23. Walton, G. and M.S. Diederichs. 2015. A new model for the dilation of brittle rocks based on laboratory compression test data with separate treatment of dilatancy mobilization and decay. *Geotechnical and Geological Engineering*. 33(3): 661-679.
24. Walton, G., M.S. Diederichs, A. Punkkinen, and J. Whitmore. 2016. Back analysis of a pillar monitoring experiment at 2.4 km depth in the Sudbury Basin, Canada. *International Journal of Rock Mechanics and Mining Sciences*. 85: 33-51.
25. Wang, X., and M. Cai. 2018. Modeling of brittle rock failure considering inter-and intra-grain contact failures. *Computers and Geotechnics*. 101: 224-244.